Glycosylation-dependent opsonophagocytic activity of staphylococcal protein A antibodies

Xinhai Chen[a,b], Miaomiao Shi[a,b], Xin Tong[c], Hwan Keun Kim[a,b,1], Lai-Xi Wang[c], Olaf Schneewind[a,b,2], and Dominique Missiakas[a,b,3]

[a]Howard Taylor Ricketts Laboratory, Argonne National Laboratory, Lemont, IL 60439; [b]Department of Microbiology, The University of Chicago, Chicago, IL 60637; and [c]Department of Chemistry and Biochemistry, University of Maryland, College Park, MD 20742

Edited by Richard P. Novick, New York University School of Medicine, New York, NY, and approved August 4, 2020 (received for review February 25, 2020)

Antibodies may bind to bacterial pathogens or their toxins to control infections, and their effector activity is mediated through the recruitment of complement component C1q or the engagement with Fcγ receptors (FcγRs). For bacterial pathogens that rely on a single toxin to cause disease, immunity correlates with toxin neutralization. Most other bacterial pathogens, including *Staphylococcus aureus*, secrete numerous toxins and evolved multiple mechanisms to escape opsonization and complement killing. Several vaccine candidates targeting defined surface antigens of *S. aureus* have failed to meet clinical endpoints. It is unclear that such failures can be solely attributed to the poor selection of antibody targets. Thus far, studies to delineate antibody-mediated uptake and killing of Gram-positive pathogens remain extremely limited. Here, we exploit 3F6-hIgG1, a human monoclonal antibody that binds and neutralizes the abundant surface-exposed Staphylococcal protein A (SpA). We find that galactosylation of 3F6-hIgG1 that favors C1q recruitment is indispensable for opsonophagocytic killing of staphylococci and for protection against bloodstream infection in animals. However, the simple removal of fucosyl residues, which results in reduced C1q binding and increased engagement with FcγR, maintains the opsonophagocytic killing and protective attributes of the antibody. We confirm these results by engineering 3F6-hIgG1 variants with biased binding toward C1q or FcγRs. While the therapeutic benefit of monoclonal antibodies against infectious disease agents may be debatable, the functional characterization of such antibodies represents a powerful tool for the development of correlates of protection that may guide future vaccine trials.

monoclonal antibody | glycosylation | C1q | FcγR | Staphylococcal protein A

Staphylococcus aureus (MSSA, methicillin-sensitive *S. aureus*) and its antibiotic-resistant isolates (MRSA, methicillin-resistant *S. aureus*) persistently colonize the nasopharynx of 31% (MSSA) and 2% (MRSA) of the US population, respectively, while the remainder population is intermittently colonized (1, 2). Colonization is the key risk factor for invasive diseases, which manifest as skin and soft-tissue infections, osteomyelitis, pneumonia, septic arthritis, bacteremia, and endocarditis (3). In the United States, community-acquired disease is associated with 3.2 million (MSSA) and 238,000 (MRSA) clinical visits each year (4). Further, 359,000 MSSA and 101,000 MRSA cases of hospital-acquired infection occur, for 37 million hospital admissions (5). MRSA infection is associated with treatment failure and increased mortality (6). Several attempts to develop vaccines or immune therapeutics that prevent disease or improve the outcome of *S. aureus* infections have failed (7).

S. aureus is a Gram-positive organism with a thick envelope, which, unlike most Gram-negative bacteria, cannot be lysed by complement and the membrane attack complex (7). Secreted Sbi and cell wall-bound SpA capture the fragment-crystallizable region of IgG (Fcγ) and thwart opsonization with *S. aureus*-specific antibodies. Sbi and SpA encompass two and five immunoglobulin-binding domains (IgBDs), respectively. Each IgBD binds to Fcγ of human IgG1, IgG2, and IgG4 (but not to IgG3) and of mouse IgG (IgG1, IgG2a, IgG2b, IgG2c, and IgG3) (8–11). SpA, but not Sbi, also binds the variant heavy chain of V_H3 idiotypic IgM, IgG, IgD, and IgE (12–14). During infection, *S. aureus* releases SpA, which cross-links the variant heavy chains of V_H3 clan B cell receptors (IgM) and triggers B cell proliferation and the secretion of V_H3 clonal antibodies (15, 16). Released SpA diverts B cell development and blocks the production of pathogen-specific IgG (15, 16). Humans, guinea pigs, and mice fail to generate SpA-neutralizing antibodies (12, 16, 17). Thus, any therapeutic strategy involving *S. aureus*-specific antibody must address the SpA and Sbi defenses of staphylococci.

Earlier, we developed nontoxigenic SpA_{KKAA} that no longer binds immunoglobulins (12) and isolated the mouse hybridoma monoclonal antibody 3F6 (3F6-mhIgG2a). This antibody binds the folded triple-helical structure of IgBDs and blocks ligand binding to SpA and Sbi. When administered to mice, 3F6-mhIgG2a protects animals against *S. aureus* bloodstream infection (11, 12, 18). In an effort to develop a therapeutic antibody, the complementarity-determining regions (CDRs) of 3F6-mhIgG2a were stitched into the VH and VL gene elements of a human IgG1 (hIgG1) antibody (18, 19) (Fig. 1*A*). The new humanized 3F6 IgG1 antibody (3F6-hIgG1) improved the outcome of MRSA bloodstream infections in experimental animals (18, 19). Here, we use a combination of

Significance

All currently licensed antibodies against bacteria target exotoxins. For most pathogens, neutralization of toxin(s) is not sufficient to prevent bacterial replication. Antibodies against surface determinants represent better candidates to enhance opsonophagocytic killing, but the mechanisms of action of such antibodies have not been systematically studied. Staphylococcal protein A is a conserved surface protein of *Staphylococcus aureus* and a crucial virulence determinant that manipulates B-cell responses and blocks deposition of opsonin. Monoclonal antibodies directed against SpA represent potential therapeutic agents as well as a formidable tool to identify and optimize effector functions of antibodies that can promote bacterial clearance.

Author contributions: X.C., H.K.K., L.-X.W., O.S., and D.M. designed research; X.C., M.S., X.T., and H.K.K. performed research; X.C., X.T., and L.-X.W. contributed new reagents/analytic tools; X.C., M.S., X.T., H.K.K., L.-X.W., O.S., and D.M. analyzed data; and X.C., L.-X.W., and D.M. wrote the paper.

Competing interest statement: D.M. declares a competing financial interest as the inventor of patents describing therapeutic antibodies against *S. aureus*.

This article is a PNAS Direct Submission.

This open access article is distributed under Creative Commons Attribution-NonCommercial-NoDerivatives License 4.0 (CC BY-NC-ND).

[1]Present address: Department of Microbiology and Immunology, Stony Brook University, Stony Brook, NY 11794.

[2]Deceased May 26, 2019.

[3]To whom correspondence may be addressed. Email: dmissiak@bsd.uchicago.edu.

This article contains supporting information online at https://www.pnas.org/lookup/suppl/doi:10.1073/pnas.2003621117/-/DCSupplemental.

First published August 27, 2020.

Downloaded at Palestinian Territory, occupied on December 30, 2021

www.manaraa.com

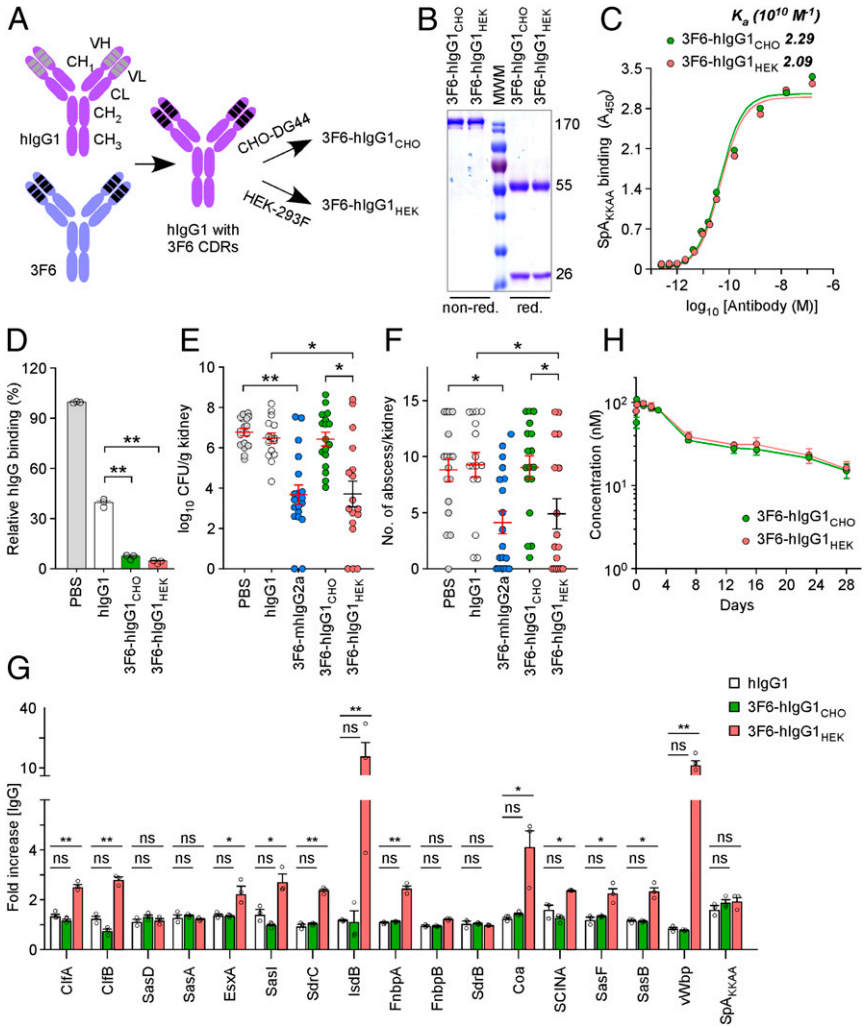

Fig. 1. 3F6-hIgG1 produced by HEK 293F cells protects mice against MRSA bloodstream infection. (*A*) Schematic of recombinant antibodies generated by swapping the complementarity determining regions (CDRs) of human V_H1-idiotypic IgG1 with the CDRs of mouse hybridoma 3F6-mhIgG2a. Production in CHO-DG44 and HEK 293F cells yielded 3F6-hIgG1$_{CHO}$ and 3F6-hIgG1$_{HEK}$, respectively. (*B*) Coomassie-stained gel of antibodies. nonred./red., nonreducing/reducing conditions, respectively. (*C*) Antibody binding to SpA$_{KKAA}$ measured by ELISA and reported as association constants (K_a; $n = 3$); A_{450}, absorbance at 450 nm. (*D*) Antibodies 3F6-hIgG1$_{CHO}$ and 3F6- hIgG1$_{HEK}$ prevent the association of SpA to human IgG better than human IgG1 (hIgG1). Values were normalized to SpA interaction with human IgG in PBS ($n = 3$). (*E* and *F*) Animals (BALB/c) received PBS, human IgG1 (hIgG1), mouse hybridoma monoclonal antibody 3F6-mhIgG2a, 3F6- hIgG1$_{CHO}$, or 3F6-hIgG1$_{HEK}$ prior to challenge with *S. aureus* MW2. Fifteen days post infection, kidneys ($n = 16$ to 20 from 2 independent experiments) were removed and either ground for enumeration of CFU per gram tissue (*E*) or fixed and stained for enumeration of internal abscesses (*F*). (*G*) Administration of 3F6-hIgG1$_{HEK}$ prior to infection promotes enhanced antistaphylococcal serum IgG responses. Sera ($n = 3$) of animals shown in *E* were tested for antibodies against the indicated *S. aureus* antigens. (*H*) Plasma concentration–time profile of antibodies following i.p. administration into BALB/c mice ($n = 5$). Data are presented as mean ± SEM (*C*–*H*). Significant differences were identified with the two-tailed Student's *t* test (*D* and *G*) and one-way ANOVA with Kruskal–Wallis test (*E* and *F*; $^{**}P < 0.01$; $^{*}P < 0.05$; ns, not significant).

glycoengineering and site-directed mutagenesis to discern the effector functions of 3F6 therapeutic antibodies.

Results

3F6-hIgG1$_{HEK}$, but Not 3F6-hIgG1$_{CHO}$, Protects Mice Against *S. aureus* Bloodstream Infection. Two cell lines, CHO-DG44 and HEK-293F, were used to produce humanized anti-SpA antibodies. The corresponding antibodies, designated 3F6-hIgG1$_{CHO}$ and 3F6-hIgG1$_{HEK}$ (Fig. 1*A*), were affinity-purified, and their integrity and homogeneity were documented by Coomassie-stained SDS/polyacrylamide gel electrophoresis (SDS/PAGE) under reducing and nonreducing conditions (Fig. 1*B*). Both antibodies exhibited a similar affinity for SpA$_{KKAA}$ (Fig. 1*C*) and displaced interactions between hIgG and SpA more effectively than hIgG1 (Fig. 1*D*). When incubated with staphylococci, ~13,400 molecules of antibody (3F6-hIgG1$_{CHO}$ or 3F6-hIgG1$_{HEK}$) were found to coat each bacterial cell (*SI Appendix*, Fig. S1). To assess their therapeutic activity, 3F6-hIgG1$_{CHO}$ and 3F6-hIgG1$_{HEK}$ were injected into BALB/c mice prior to i.v. challenge with the methicillin-resistant *S. aureus* isolate MW2, herein referred to as MRSA (Fig. 1 *E* and *F*). Animals treated with PBS and hIgG1 or with 3F6-mhIgG2a served as negative and positive control groups, respectively. Animals were killed 15 d post challenge. Disease was assessed by visual inspection of intact kidneys for areas with pus collection (*SI Appendix*, Fig. S2*A*), enumeration of colony-forming units (CFU) following plating of kidney tissues (Fig. 1*E*), and enumeration of abscess lesion using H&E-stained kidney tissue sections (Fig. 1*F*). Animals that received 3F6-mhIgG2a or 3F6-hIgG1$_{HEK}$ harbored fewer abscess lesions (*SI Appendix*, Fig. S2*A* and Fig. 1*F*) and reduced bacterial loads in renal tissues (Fig. 1*E*) compared to animals that received PBS or hIgG1.

Downloaded at Palestinian Territory, occupied on December 30, 2021

www.manaraa.com

The protective activities of 3F6-mhIgG2a and 3F6-hIgG1$_{HEK}$ were indistinguishable. Surprisingly, 3F6-hIgG1$_{CHO}$ administration afforded no protection and behaved similarly to PBS and hIgG1 controls (*SI Appendix*, Fig. S2*A* and Fig. 1 *E* and *F*). Earlier reports demonstrate that successful neutralization of SpA blocks its B cell superantigen activity, resulting in the production of polyclonal antibodies against staphylococcal antigens (12, 18). Animal sera collected postchallenge were used to measure IgG titers against a staphylococcal antigen matrix encompassing 17 purified antigens (Fig. 1*G*). Immunization with 3F6-hIgG1$_{HEK}$ or reference control 3F6-mhIgG2a elicited antibody production against the virulence determinants ClfA, IsdB, Coa, and vWbp as well as surface antigens ClfB, SasI, and FnBPA; this was not observed in animals treated with 3F6-hIgG1$_{CHO}$, PBS, or hIgG1 (Fig. 1*G* and *SI Appendix*, Fig. S2*B*). i.p. injection of 3F6-hIgG1$_{CHO}$ and 3F6-hIgG1$_{HEK}$ into mice was associated with a typical biexponential plasma concentration–time profile, revealing similar half-lives (Fig. 1*H*). In agreement with this observation, 3F6-hIgG1$_{CHO}$ and 3F6-hIgG1$_{HEK}$ displayed similar binding affinities to the human neonatal Fc receptor (FcRn) in vitro (*SI Appendix*, Fig. S2*C*). Together these data indicate that 3F6-hIgG1$_{HEK}$, but not 3F6-hIgG1$_{CHO}$, protects mice against MRSA infection, and the difference in protection is not caused by a reduced half-life of 3F6-hIgG1$_{CHO}$. To determine when 3F6-hIgG1$_{HEK}$ protected animals during infection, antibodies were transferred 24 h before or 24 h after infection, and animals were killed 5 and 15 d following bloodstream inoculation with MRSA (*SI Appendix*, Fig. S2 *D* and *E*). Staphylococci disseminate to organs and begin to replicate into foci that mature to H&E-stainable lesions over 5 d. Prior administration of 3F6-hIgG1$_{HEK}$ caused a significant reduction in bacterial loads on day 5 compared to mock ($1.72 \times 10^8 \pm 2.43 \times 10^7$ vs. $8.61 \times 10^7 \pm 1.40 \times 10^7$ CFU/g kidney) but no reduction in the number of lesions (*SI Appendix*, Fig. S2 *D* and *E*). This 50% reduction in bacterial loads supports the notion that the antibody promotes opsonophagocytic killing. As expected, on day 15 post infection, both bacterial loads and abscess lesions were significantly reduced (*SI Appendix*, Fig. S2 *D* and *E*). As neutralization of the B cell superantigen activity of SpA elicits a broad antibody response (Fig. 1*G*), the continued clearance of bacteria is likely due to both monoclonal and polyclonal antibodies. Administration of 3F6-hIgG1$_{HEK}$ post infection also protected animals, but significant differences were only observed on day 15 for bacterial loads in kidneys (*SI Appendix*, Fig. S2 *D* and *E*).

Fc-Galactosylation Is Required for the Protective Activity of 3F6 Antibodies. Antibody-mediated effector functions are modulated by Fc N-glycosylation (20). Asn^{297} is modified with a heptasaccharide core ($GlcNAc_2Man_3GlcNAc_2$) and variable additions of fucose (F), galactose (G), and sialic acid (S). Binding to the immobilized *Erythrina crista-galli* lectin (ECL) and *Sambucus nigra* agglutinin (SNA) suggested that 3F6-hIgG1$_{HEK}$ has higher galactose and sialic acid contents than 3F6-hIgG1$_{CHO}$ (*SI Appendix*, Fig. S3 *A* and *B*). For a more thorough analysis, glycans were released from antibody preparations and subjected to matrix-assisted laser desorption/ionization time-of-flight (MALDI-TOF) mass spectrometry to reveal a complex carbohydrate content profile with peaks corresponding to the fucosylated nongalactosylated (G0F), monogalactosylated (G1F), and digalactosylated N-glycans (G2F; Fig. 2*A*). The G1F and G2F glycoforms were more abundant in the 3F6-hIgG1$_{HEK}$ preparation compared to the 3F6-hIgG1$_{CHO}$ preparation (Fig. 2 *A* and *B*). Quantification of glycoforms revealed that 3F6-hIgG1$_{HEK}$ contains two times and nine times more galactosyl and sialic acid residues, respectively, than 3F6-hIgG1$_{CHO}$ (Fig. 2*B* and *SI Appendix*, Table S1). To determine whether the Fc glycan structure is a key determinant for protection against *S. aureus* bloodstream infection, we used enzymes to transfer or remove galactose, yielding 3F6-hIgG1$_{CHO}$-Gal or 3F6-hIgG1$_{HEK}$-deGal. Neuraminidase was used to generate 3F6-hIgG1$_{CHO}$-deSia and 3F6-hIgG1$_{HEK}$-deSia lacking sialic acid. None of these treatments altered the integrity of antibodies (*SI Appendix*, Fig. S3 *C* and *F*). These glycoforms bound SpA$_{KKAA}$ with similar affinities (Table 1 and *SI Appendix*, Fig. S3 *D* and *G*). Lectin binding assays confirmed the galactosylation, degalactosylation, or desialylation modifications of antibodies (*SI Appendix*, Fig. S3 *E* and *H*). Animals were injected intraperitoneally with the five test antibodies, 3F6-hIgG1$_{CHO}$, 3F6-hIgG1$_{CHO}$-Gal, 3F6-hIgG1$_{HEK}$, 3F6-hIgG1$_{HEK}$-deGal, or 3F6-hIgG1$_{HEK}$-deSia, and then challenged by i.v. inoculation of MRSA while monitoring body weight changes over 14 d (Fig. 2*C*). On day 15, animals were euthanized and renal tissues examined for bacterial load and abscess formation (Fig. 2 *D* and *E*). As shown earlier, treatment with 3F6-hIgG1$_{HEK}$ but not human IgG1 and 3F6-hIgG1$_{CHO}$ reduced MRSA load as well as abscess formation (Fig. 2 *D* and *E*). Sialic acid modification (3F6-hIgG1$_{HEK}$-deSia) is not required for this protective activity, while galactosylation is indispensable, as demonstrated by the loss of protection upon treatment of animals with 3F6-hIgG1$_{HEK}$-deGal and by the gain of protection upon passive administration with 3F6-hIgG1$_{CHO}$-Gal (Fig. 2 *C*–*E*). To unambiguously identify the Fc glycan structure responsible for protection against MRSA bloodstream infection, we used a chemoenzymatic method for glycan remodeling by first deglycosylating 3F6-hIgG1$_{CHO}$ and 3F6-hIgG1$_{HEK}$ with Endo-S2 and, second, transferring presynthesized glycan en bloc from activated glycan oxazoline in an EndoS2-D184M–dependent manner (21–24). Four antibodies, 3F6-hIgG$_{HEK}$-G0F, 3F6-hIgG$_{HEK}$-G1F, 3F6-hIgG$_{HEK}$-G2F, and 3F6-hIgG$_{CHO}$-G2F, with highly homogeneous and well-defined glycan profiles, were synthesized and tested for integrity and binding to SpA$_{KKAA}$ (*SI Appendix*, Fig. S3 *I* and *J* and Table 1). When injected in animals, both digalactosylated antibodies, 3F6-hIgG$_{HEK}$-G2F and 3F6-hIgG$_{CHO}$-G2F, protected animals from MRSA challenge (Fig. 2 *F*–*H*). Monogalactosylated 3F6-hIgG$_{HEK}$-G1F protected equally well. However, no protection was observed for the G0F glycoform 3F6-hIgG1$_{HEK}$-G0F (Fig. 2 *F*–*H*). 3F6 antibody-mediated protection correlated with the development of a broader immune response against multiple bacterial molecules as monitored with the MRSA antigen matrix (Fig. 2 *I* and *J*). In conclusion, galactosylation is key to the protective attribute of 3F6-hIgG1 in vivo.

Protection by 3F6-hIgG1$_{HEK}$ in Mice Requires Complement. C1q and FcγR interactions are both impacted by antibody galactosylation at Asn^{297} (25, 26). 3F6-hIgG1$_{HEK}$ displayed a greater affinity for both human and mouse C1q than 3F6-hIgG1$_{CHO}$ (*SI Appendix*, Fig. S4 *A* and *B* and Table 1). The differential glycosylation of CHO- and HEK-produced antibodies did not affect their binding affinities toward mouse FcγRs (*SI Appendix*, Fig. S4*C* and Table 2). When examined using human FcγRs and their allotypes, 3F6-hIgG1$_{CHO}$ showed higher affinity toward activating receptors FcγRIIA$_{R131}$, FcγRIIA$_{H131}$, FcγRIIIA$_{V158}$, and FcγRIIIA$_{F158}$ and the inhibitory receptor FcγRIIB compared to 3F6-hIgG1$_{HEK}$ (*SI Appendix*, Fig. S4*D* and Table 2). Both antibodies bound FcγRIA similarly (*SI Appendix*, Fig. S4*D* and Table 2). Addition of galactose to CHO-produced antibody enhanced C1q binding, while removal of galactose from HEK-produced antibody reduced C1q binding (*SI Appendix*, Fig. S4*E* and Table 1). 3F6-hIgG1$_{CHO}$-G2F displayed the highest affinity toward C1q, comparable to that of 3F6-hIgG1$_{HEK}$-G2F (*SI Appendix*, Fig. S4*F* and Table 1). Glycoforms 3F6-hIgG1$_{HEK}$-G1F and 3F6-hIgG1$_{HEK}$-G2F displayed high affinities toward C1q (*SI Appendix*, Fig. S4*F* and Table 1). Last, removal of sialic acid from 3F6-hIgG1$_{HEK}$ improved C1q binding slightly but had no impact on 3F6-hIgG1$_{CHO}$ activity (*SI Appendix*, Fig. S4*G* and Table 1). This is unsurprising since sialic acid is only added to galactose residues; thus, only 0.45% of all

Downloaded at Palestinian Territory, occupied on December 30, 2021
www.manaraa.com

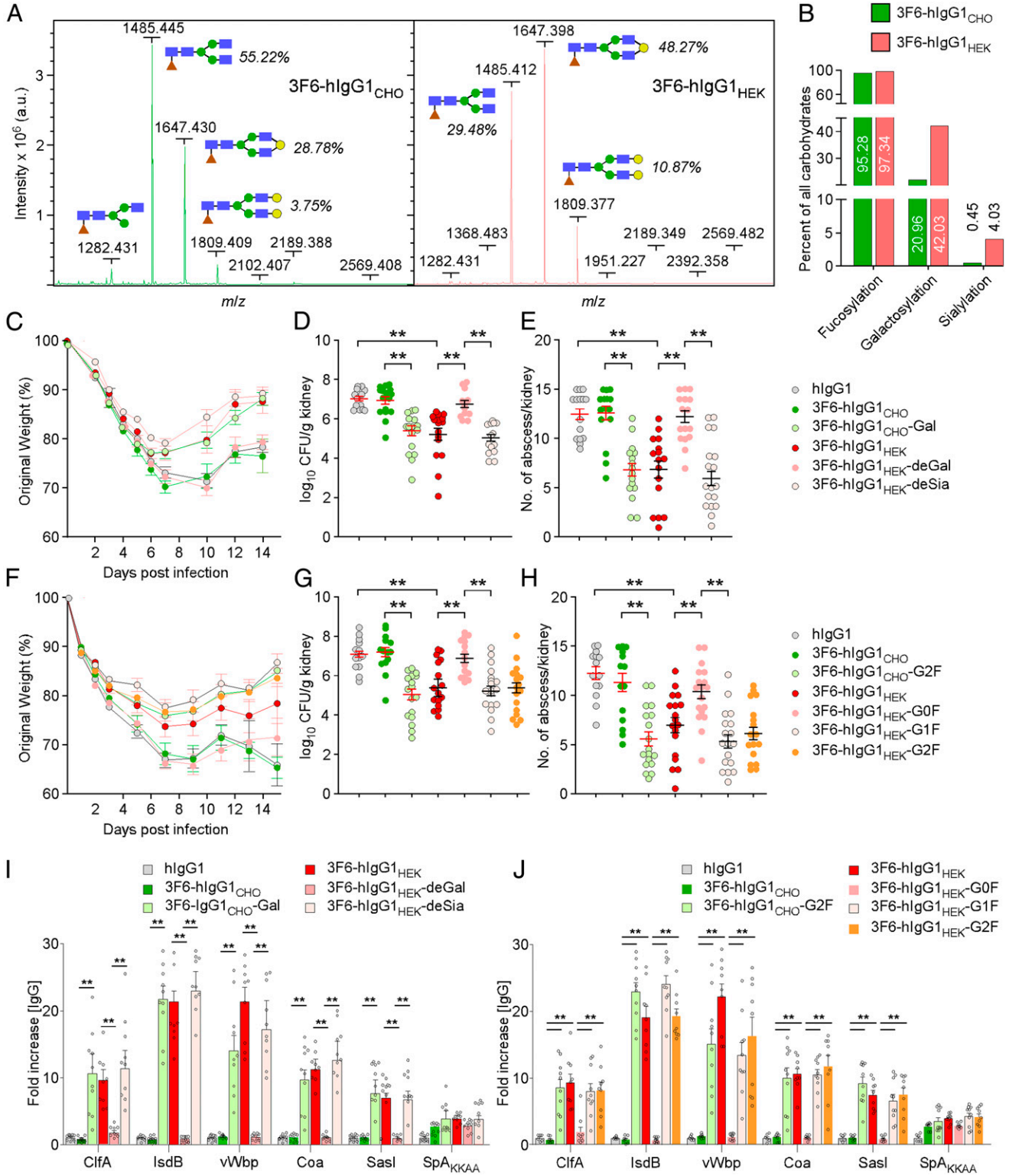

Fig. 2. 3F6-hIgG1 glycoforms are determinants of therapeutic efficacy against MRSA. (*A*) MALDI-TOF mass spectra of 3F6-hIgG1$_{CHO}$ (*Left*) and 3F6-hIgG1$_{HEK}$ (*Right*) with glycan structures: fucose (brown), N-acetylglucosamine (blue), mannose (green), and galactose (yellow). (*B*) Quantification of glycoforms from mass spectra shown in *A*. (*C–J*) Animals (BALB/c) received test antibodies as indicated before challenge with *S. aureus* MW2. Weight (n = 10) was recorded daily and reported as percentage of initial weight (*C* and *F*). Fifteen days post infection, kidneys and sera were obtained during necropsy as described in Fig. 1; kidneys (n = 16 to 20 from 2 independent experiments) were examined for CFU (*D* and *G*) and internal abscesses (*E* and *H*), and animal sera (n = 6 to 10) were tested for antibodies against the indicated *S. aureus* antigens (*I* and *J*). Data are presented as mean ± SEM (*C–J*). Significant differences were identified with one-way ANOVA with Kruskal–Wallis test (*D–G*) and the two-tailed Student's t test (*I* and *J*; $^{**}P < 0.01$; $^{*}P < 0.05$; ns, not significant).

MICROBIOLOGY
Downloaded at Palestinian Territory, occupied on December 30, 2021
www.manaraa.com

Table 1. Association constants for the binding of glycoengineered 3F6-hIgG1 to ligands measured by ELISA

		3F6-hIgG1$_{CHO}$			
Ligand	K_a, M^{-1}	WT	Gal	deSia	G2F
SpA_{KKAA}	10^{10}	2.54 ± 0.46	2.74 ± 0.23	2.85 ± 0.33	1.93 ± 0.13
Human C1q	10^6	4.91 ± 0.24	21.7 ± 1.71	5.50 ± 0.15	51.1 ± 6.57
Mouse C1q	10^6	8.87 ± 0.59	ND	ND	ND

		3F6-hIgG1$_{HEK}$					
Ligand	K_a (M^{-1})	WT	deGal	deSia	G0F	G1F	G2F
SpA_{KKAA}	10^{10}	2.44 ± 0.52	2.86 ± 0.33	2.90 ± 0.32	2.34 ± 0.13	2.24 ± 0.16	1.93 ± 0.16
Human C1q	10^6	18.7 ± 4.0	4.0 ± 0.70	33.7 ± 3.74	6.94 ± 0.39	38.3 ± 3.58	55.0 ± 6.03
Mouse C1q	10^6	60.8 ± 7.44	ND	ND	ND	ND	ND

WT, wild-type; Gal, galactosylated; deSia, desialylated; ND, not determined; deGal, degalactosylated.

CHO-produced antibodies were modified with sialic acid, compared to ~4% of all HEK-produced antibodies (Fig. 2*B*). To rule out the possibility that glycosylation may favor hexamer formation of antibodies (hexabodies), glycoforms of 3F6-hIgG1$_{CHO}$ and 3F6-hIgG1$_{HEK}$ antibodies were incubated with human serum. Hexabodies have been shown to bind C1q spontaneously and to activate complement in the absence of antigen (27). Complement activation assessed as increased C4d formation was only observed in the presence of heat-aggregated human IgG (HAG); neither 3F6 antibodies purified from CHO or HEK cells nor the chemoenzymatically modified variants elicited C4d production in serum (*SI Appendix*, Fig. S4*H*).

Amino acids K322 and L233/L234 have been implicated in the interaction of antibody with C1q (28, 29). To further delineate the C1q requirement for the therapeutic activity of 3F6-hIgG1$_{HEK}$ antibodies, we generated variants 3F6-hIgG1$_{HEK}$-KA and 3F6-hIgG1$_{HEK}$-LALA with substitutions K322A and L233A/L234A, respectively (*SI Appendix*, Fig. S5*A*). These substitutions did not affect antigen binding, sialylation, fucosylation, or galactosylation (*SI Appendix*, Fig. S5 *B* and *C* and Table 2). Binding to both human and mouse C1q was significantly reduced for these two variants, with affinities even lower than that of 3F6-hIgG1$_{CHO}$ for human and mouse C1q (*SI Appendix*, Fig. S5*D* and Table 2). 3F6-hIgG1$_{HEK}$ and the KA variant interacted similarly with recombinant human FcγRs, but the LALA variant was impaired for interaction with human FcγRIA and FcγRIIIA$_{V158}$ (*SI Appendix*, Fig. S5*E* and Table 2). The KA variant exhibited slightly higher affinity to all mouse FcγRs compared to 3F6-hIgG1$_{HEK}$; the LALA variant interacted considerably less well with mouse FcγRI and FcγRIV (*SI Appendix*, Fig. S5*F* and Table 2). When administered to animals, the KA and LALA variants failed to restore body weight or reduce bacterial burden and abscesses in tissues 15 d postinfection with MRSA, revealing an inability to clear bacteria (Fig. 3 *A*–*C*). The KA and LALA variants also failed to neutralize the B cell superantigen activity of SpA, as reflected by the lack of a broad neutralizing antibody response (*SI Appendix*, Fig. S5*G*). Collectively, these findings indicate that C1q recruitment may be key to the therapeutic activity of anti-MRSA antibodies.

FcγRs Contribute to the Therapeutic Activity of 3F6-hIgG1$_{HEK}$. Antibody interaction with FcγRs can be modulated by fucosylation. Loss of fucosylation results in weaker and higher binding toward inhibitory and activating FcγRs, respectively (30). 3F6-hIgG1$_{HEK}$ is extensively fucosylated (Fig. 2*B*), a modification that may not be optimal for FcγR-mediated activity. To test this possibility, afucosylated 3F6-hIgG1$_{HEK}$ (3F6-hIgG1$_{HEK}$-afu) was produced by adding kifunensine to the culture medium in an effort to enrich for low-fucose glycoforms. 3F6-hIgG1$_{HEK}$-afu retained its

Table 2. Association constants for the binding of 3F6-hIgG1$_{CHO}$ or 3F6-hIgG1$_{HEK}$ variants to ligands measured by ELISA

			3F6-hIgG1$_{HEK}$			
Ligand	K_a, M^{-1}	WT 3F6-hIgG1$_{CHO}$	WT	KA	LALA	afu
SpA_{KKAA}	10^{10}	2.54 ± 0.46	2.44 ± 0.52	2.85 ± 0.26	2.94 ± 032	2.50 ± 0.25
Human						
C1q	10^6	4.91 ± 0.24	18.7 ± 4.0	1.37 ± 0.62	2.04 ± 1.18	5.97 ± 0.31
FcγRIA	10^8	7.66 ± 1.35	7.88 ± 1.51	7.86 ± 1.89	0.026 ± 0.086	5.83 ± 4.15
FcγRIIA (R131)	10^6	2.36 ± 0.39	1.53 ± 0.18	1.81 ± 0.18	0.99 ± 0.11	1.82 ± 0.25
FcγRIIA (H131)	10^6	1.75 ± 0.30	1.13 ± 0.16	1.23 ± 0.28	0.46 ± 0.029	1.51 ± 0.46
FcγRIIB	10^5	16.5 ± 1.92	9.25 ± 2.23	11.8 ± 1.55	8.38 ± 2.45	1.79 ± 0.88
FcγRIIIA (V158)	10^7	2.75 ± 0.50	2.31 ± 0.44	1.40 ± 0.12	0.26 ± 0.14	5.63 ± 0.94
FcγRIIIA (F158)	10^6	3.09 ± 0.33	1.97 ± 0.25	1.51 ± 0.34	0.85 ± 0.18	9.20 ± 0.14
Mouse						
C1q	10^6	8.87 ± 0.59	60.8 ± 7.44	1.34 ± 0.30	2.91 ± 0.12	2.79 ± 0.16
FcγRI	10^8	1.77 ± 0.44	1.84 ± 0.48	3.97 ± 0.34	0.021 ± 0.078	0.92 ± 0.094
FcγRIIB	10^6	1.53 ± 0.26	1.61 ± 0.21	3.35 ± 0.48	1.60 ± 0.18	1.62 ± 0.12
FcγRIII	10^6	1.49 ± 0.16	1.69 ± 0.19	2.96 ± 0.40	1.72 ± 0.21	2.30 ± 0.34
FcγRIV	10^8	1.15 ± 0.20	1.35 ± 0.43	2.66 ± 0.88	0.09 ± 0.019	3.19 ± 0.38

WT, wild-type; KA, K322A substitution; LALA, L233A/L234A substitutions; afu, afucosylated.

Downloaded at Palestinian Territory, occupied on December 30, 2021

www.manaraa.com

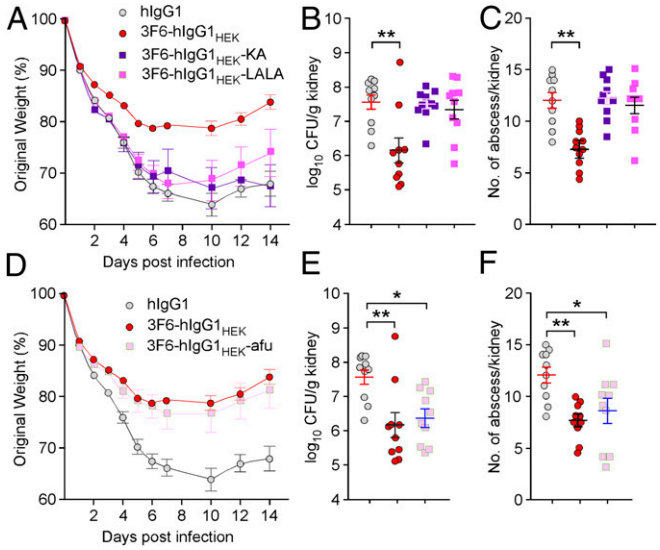

Fig. 3. Contribution of complement and FcγRs to 3F6-hIgG1$_{HEK}$–mediated protection against MRSA bloodstream infection. (*A–C*) Animals (BALB/c; n = 10 from 2 independent experiments) received control hIgG1, 3F6-hIgG1$_{HEK}$, 3F6-hIgG1$_{HEK}$-KA, or 3F6-hIgG1$_{HEK}$-LALA before challenge with *S. aureus* MW2. Disease was assessed as described in Fig. 1. (*D–F*) Animals (BALB/c; n = 10 from 2 independent experiments) were treated with control hIgG1, 3F6-hIgG1$_{HEK}$, or 3F6-hIgG1$_{HEK}$-afu antibodies prior to challenge with *S. aureus* MW2. Disease was assessed as described in Fig. 1. Data are presented as mean ± SEM. Significant differences were identified with one-way ANOVA with Kruskal–Wallis test (**P < 0.01; *P < 0.05). One of two repeats is shown.

integrity and SpA$_{KKAA}$ binding (*SI Appendix*, Fig. S6 *A* and *B*). Lectin-based assays confirm the low-level fucosylation and galactosylation of 3F6-hIgG1$_{HEK}$-afu compared to 3F6-hIgG1$_{HEK}$ (*SI Appendix*, Fig. S6*C*). Binding to inhibitory receptor human FcγRIIB was reduced, and binding to activating receptors human FcγRIIIA (both alleles) and mouse FcγRIII and FcγRIV was enhanced (*SI Appendix*, Fig. S6 *D–F* and Table 2), thus effectively altering the activating-to-inhibitory (A/I) ratio of FcγRs (31). Importantly, 3F6-hIgG1$_{HEK}$-afu displayed significantly reduced affinity for human and mouse C1q compared to fucosylated 3F6 (Table 2). In fact, 3F6-hIgG1$_{HEK}$-afu interactions with C1q molecules were as weak as that of nontherapeutic 3F6-hIgG1$_{CHO}$ (Table 2). Nonetheless, when transferred to animals, 3F6-hIgG1$_{HEK}$-afu controlled MRSA infection as reflected by the reduced weight loss, bacterial loads, and abscesses and the broad antibody responses against secreted antigens (Fig. 3 *D–F* and *SI Appendix*, Fig. S6*G*). Thus, we attribute the protective activity of 3F6-hIgG1$_{HEK}$-afu in animals to its enhanced binding toward activating FcγRs. These results suggest that the therapeutic activity of 3F6-hIgG1$_{HEK}$ may be achieved both in complement- and FcγRs-dependent manners in vivo.

Both Complement and FcγRs Contribute to the OPK Activity of 3F6-hIgG1$_{HEK}$ in Human Blood. In addition to capturing immunoglobulins in an SpA- and Sbi-dependent manner, *S. aureus* also exploits the host factors prothrombin and fibrinogen to induce the formation of fibrin agglutinates that shield bacteria from phagocytes. Secreted coagulases, Coa and vWbp, and surface-displayed ClfA are key factors involved in this process (32). Correlates of protection for vaccines are typically measured as the concentration of antibody able to induce opsonophagocytosis of a given pathogen by HL60 cells, i.e., human promyelocytic leukemia cells (33). Because this assay lacks hemostasis factors (prothrombin and fibrinogen), it is not adequate to evaluate the opsonophagocytic activity of antibodies against *S. aureus*. Earlier work developed a whole-blood assay whereby enumeration of *S. aureus* after 1 h incubation in freshly drawn anticoagulated blood is achieved by releasing bacteria from agglutinates upon treatment with the plasminogen activator streptokinase (32). Using this assay, 3F6-hIgG1$_{HEK}$ promoted killing of MRSA in human blood. As expected, pretreatment of blood with cytochalasin D, an inhibitor of actin polymerization and thus phagocytosis, abrogated 3F6-hIgG1$_{HEK}$–mediated killing of MRSA in human blood (Fig. 4*A*). Pretreatment of blood with C1 esterase inhibitor (C1-inh) that binds and inactivates C1r and C1s also prevented killing of bacteria in the presence of 3F6-hIgG1$_{HEK}$ antibodies. Antibody binding to C1q activates C1r and C1s to trigger the classical complement pathway and the activation of C3 and C5 (34). In agreement with a requirement for complement, neither the KA nor the LALA variant of 3F6-hIgG1$_{HEK}$ promoted opsonophagocytic killing. Nonetheless, afucosylated 3F6-hIgG1$_{HEK}$ with greatly reduced C1q binding and enhanced FcγR binding activity promoted the killing of MRSA in human blood (Fig. 4*C*). Thus, in this opsonophagocytic assay optimized for coagulase-positive *S. aureus*, bacterial killing may be promoted by both effector functions of antibody.

Discussion

The discovery that serum from infected animals contains antibacterial activity was readily exploited in the early 20th century, principally against diphtheria toxin (35). Broader-spectrum drugs and antibiotics soon eclipsed serum therapy. To date, only a handful of therapeutic antibodies have been licensed for the prevention of infectious diseases (36). This is unlike the expanding number of mAbs for immune-mediated disorders and cancer (37). While target selection through Fab recognition is critical for success, disease amelioration is governed by the deployment of effector mechanisms mediated by the Fc regions of antibodies. Effector functions have been best characterized for anticancer antibodies for which the specific destruction of tumor cells or the enhancement of tumor-specific T cell immunity can be readily measured (38, 39). Interactions with FcγRs trigger antibody-dependent cell-mediated cytotoxicity (ADCC) and antibody-dependent cell mediated phagocytosis (ADCP) of tumor cells (38, 39). Interaction with

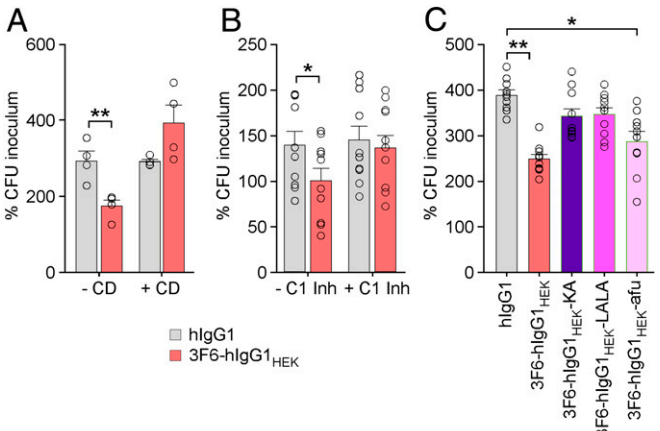

Fig. 4. 3F6-hIgG1$_{HEK}$ employs both complement and FcγRs to promote opsonophagocytic killing in human blood. (*A*) *S. aureus* MW2 survival in human blood (n = 4) without or with cytochalasin D (–/+ CD). (*B*) *S. aureus* MW2 survival in human blood (n = 5) in absence or presence of complement inhibitor (–/+ C1 Inh). (*C*) Opsonophagocytic killing activities of antibody variants compared to hIgG1 and 3F6-hIgG1$_{HEK}$ toward *S. aureus* MW2 in human blood (n = 10). Data were plotted as the average ± SEM of CFUs after 60 min incubation in blood compared to CFUs of inoculum (set as 100%). Significant differences were identified with the two-tailed Student's t test (*P < 0.05; **P < 0.01).

Downloaded at Palestinian Territory, occupied on December 30, 2021
www.manaraa.com

C1q activates the classical complement pathway to promote the direct lysis of tumor cells upon insertion of the membrane attack complex (i.e., complement-dependent cytotoxicity [CDC]) or the covalent deposition of opsonins such as C3b onto the cell surface. Complement receptors on effector cells bind opsonized targets promoting complement-dependent cell-mediated cytotoxicity (CDCC) and complement-dependent cell-mediated phagocytosis (CDCP) (40, 41). The mode of action required for antibody-mediated elimination of bacterial pathogens is not as well understood.

We have shown earlier that protection against *S. aureus* disease by candidate 3F6-hIgG1 correlates with the ability of this antibody to bind multiple IgBDs of SpA and block further interactions with Fcγ and Fab V_H3 domains of Ig (11). However, CHO cell-produced 3F6-hIgG1$_{CHO}$ displayed no therapeutic activity in a mouse model of MRSA infection. This was unlike 3F6-hIgG1 produced in HEK 293F cells. CHO cell is a nonhuman mammalian cell line, often selected for the commercial production of therapeutic proteins owing to high productivity and low operating costs (42). Lack of antibody activity could not be attributed to a reduced half-life in vivo or an inability to form immune complexes with SpA. Rather, the defect correlated with the low abundance of galactosylated antibodies in CHO cells compared to HEK 293 cells (~30% vs. ~58% G0F, ~48% vs. ~28% G1F, and ~11% vs. ~4% G2F) (43–45), suggesting altered Fc-mediated effector activity (25, 26, 46). Enzymatic addition of galactosyl residues enhanced the therapeutic activity of 3F6-hIgG1$_{CHO}$ while enzymatic degalactosylation reduced the therapeutic activity of 3F6-hIgG1$_{HEK}$. Chemoenzymatic glycoengineering further demonstrated therapeutic activity for G1F and G2F glycoforms of 3F6-hIgG1 but not for G0F.

Both the length and substitutions of N-glycans at Asn297 have been shown to affect the stability of the polypeptide loop containing Asn297 and influence binding with FcγRs and C1q (25, 26, 46). Increased galactosylation of 3F6-hIgG1 and removal of sialic acid residues enhanced both human and mouse C1q binding in vitro without altering binding to mouse FcγRs. Overall, the activating-to-inhibitory ratio (calculated by dividing the affinity of antibody for activating receptors by the affinity for inhibitory receptors) was similar between 3F6-hIgG1$_{CHO}$ and 3F6-hIgG1$_{HEK}$. These in vitro data support the notion that the therapeutic activity of galactosylated 3F6-hIgG1 is C1q-dependent. In agreement with this model, antibodies with amino acid substitutions L233A/L234A or K322A displayed reduced C1q binding and failed to protect animals from MRSA bloodstream infection. Of note, substitution K322A did not affect interactions with FcγRs at all.

SpA is extremely abundant on the surface of *S. aureus*, with ~13,400 molecules per cell. It is thus reasonable to hypothesize that the proximal binding of multiple 3F6-hIgG1-G2K molecules recruits C1q to activate the classical pathway of complement, which converges in the assembly of C3 convertase (C4b2a). C3 convertase cleaves C3 into C3a and C3b; C3b can be covalently linked to the staphylococcal surface (opsonization) while C3a acts as a chemoattractant for phagocytes. High local concentrations of C3b activate the C5 convertase, resulting in the production of the C5a chemoattractant and C5b, whose surface deposition promotes membrane attack complex formation (47). The thick peptidoglycan of *S. aureus* provides intrinsic resistance against CDC. Thus, it is likely that C3a and C5a production promote immune cell recruitment and degranulation while C3b likely promotes CDCP. In agreement with this notion, inactivation of complement C1r/C1s molecules or addition of cytochalasin D in whole human blood prevented killing of MRSA in the presence of 3F6-hIgG1. Interestingly, *S. aureus* deploys a vast array of secreted factors to block complement activation (reviewed in ref. 48). SpA and Sbi IgBDs capture antibodies in a manner that prevents further C1q but not FcγR binding (48). Sbi carries two additional domains that associate with C3 and factor H (fH) to inhibit the alternative pathway (48). In addition, staphylococcal complement inhibitor (SCIN) and homologs SCIN-B and SCIN-C inhibit C3 convertase (C3bBb). SCIN factors are encoded by many, but not all, human clinical isolates, and associate with human C3 convertase but not with other vertebrate convertases (48). Extracellular fibrinogen-binding protein (Efb) and its less conserved homolog, extracellular complement-binding protein (Ecb), bind C3d, a cleavage product of C3b that activates innate and adaptive responses by binding to complement receptor 2 (CR2). Efb and Ecb also inhibit mouse and human C3bBb and C5 convertases while Ecb facilitates fH's activity (48). Staphylokinase associates with human plasminogen to cleave many factors, including C3b and iC3b, on bacterial surfaces (48).

Our findings suggest that 3F6-hIgG1$_{HEK}$ may also engage FcγRs as long as fucosylation of N-glycans is prevented. This is in agreement with the notion that fucosylation favors interactions with C1q and inhibitory FcγRs while weakening interactions with activating FcγRs (30). CRs and FcγRs are coexpressed on immune cells and engage in cross-talk activities. For example, C5a–C5aR interaction up-regulates the expression of activating FcγRs (FcγRIII and FcγRIV) and down-regulates the expression of inhibitory FcγRIIB (49, 50). Thus, in vivo, the immediate effect of 3F6-hIgG1$_{HEK}$ may be the rapid and strong activation of complement; subsequent C–CR interactions such as C5a–C5aR may lead to an increased A/I ratio that may tip the threshold activation of FcγRs by 3F6-hIgG1$_{HEK}$.

In conclusion, our work suggests that antibodies against *S. aureus* can be improved to achieve greater therapeutic activity, especially against hard-to-treat recurrent or persistent infections caused by antibiotic-resistant strains. Importantly, a better understanding of effector functions and of pathways leading to pathogen clearance by antibodies can be exploited to define correlates of protection for candidate vaccines.

Materials and Methods

Detailed information describing materials and methods is provided in *SI Appendix, Materials and Methods*.

Bacterial Strains, Mammalian Cell Lines and Growth Media. Community-acquired methicillin-resistant *S. aureus* USA400 (MW2) was grown in tryptic soy broth or agar at 37 °C. Suspension serum-free adapted FreeStyle 293-F cells (herein referred as HEK-293F cells) were cultured in FreeStyle 293 Expression Medium (Life Technologies) and maintained in a 5% CO_2 humidified incubator at 37 °C. Kifunensine (Abcam), a small-molecule inhibitor of the enzyme α-mannosidase I, was added directly to FreeStyle 293 Expression Medium at a final concentration of 200 ng/mL (51–53).

Construction, Expression, and Purification of Recombinant 3F6-hIgG1 and Variant Antibodies. The clone encoding 3F6-hIgG1 was as described earlier (18, 19). Briefly, plasmid encoding 3F6-hIgG1 was generated by swapping the coding sequences of the heavy- and light-chain genes of the mouse monoclonal antibody 3F6-mhIgG2a (54) into the expression vector pVITRO1-102.1F10-IgG1/λ (Addgene, no. 50366). This construct served as a template for further mutagenesis. Primers 5′ TGAAGCCGCCGGGGGACCGT CAGTCTTCCT 3′ and 5′ CCCGGCGGCTTCAGGTGCTGGGCACGGTG 3′ were used to generate the LALA variant, and primers 5′ TGCGCCGTCTCCAAC AAAGCCCTCCCA 3′ and 5′ GACGGCGCACTTGTACTCCTTGCCAT 3′ were used to generate the KA variant by site-directed mutagenesis as described earlier (28). All new plasmids were transfected into HEK-293F cells using polyethylenimine (55). Candidate transfectants were selected using hygromycin B (400 μg/mL) and expanded in TripleFlask Cell Culture Flasks (Thermo Fisher). 3F6-hIgG1$_{CHO}$ was produced using the dihydrofolate reductase-deficient mutant Chinese hamster ovary cell line DG44 as described earlier (19). Antibodies were affinity-purified from supernatants of expanded cultures on protein A-Sepharose (Sigma) and dialyzed to PBS as described earlier (11).

Animal Experiments. BALB/c mice (6 to 7 wk of age) were obtained from Jackson Laboratory. For passive immunization studies, animals were injected

Downloaded at Palestinian Territory, occupied on December 30, 2021

www.manaraa.com

into the peritoneum with 5 mg/kg of indicated antibody 24 h before or 24 h after challenge. For challenge with *S. aureus*, animals were anesthetized with a mix of ketamine/xylazine (100 and 20 mg/kg). Cultures of USA400 (MW2) were grown to an absorbance at 600 nm of 0.42, and bacteria were washed in PBS once and adjusted to a suspension of 6.5×10^7 CFU/mL (colony forming unit). A total of 100 μL of this suspension was injected into the periorbital venous plexus of anesthetized animals (groups of 10 to 20). Animals were monitored for clinical signs of disease and weighed daily for 14 d. On day 15, mice were killed by carbon dioxide inhalation and necropsied to remove kidneys. Surface abscesses visible on intact kidneys were enumerated. One kidney per animal was fixed in 4% formalin for 24 h at room temperature; tissues were embedded in paraffin, thin-sectioned, stained with hematoxylin/eosin, and inspected by light microscopy to visualize and enumerate internal abscess lesions. The second kidney was weighed, homogenized, serially diluted, and plated on agar to count bacterial burden in tissues (CFU per gram of tissue). To measure the half-life of test antibodies, mice (groups of five) were injected into the peritoneal cavity with antibodies (5 mg/kg of body weight). After 1 and 4 h and after 1, 2, 3, 7, 13, 16, 23, and 28 d, periorbital venous blood was obtained and plasma samples analyzed by ELISA. Plasma antibody concentrations were calculated using a standard curve of 3F6-hIgG1$_{HEK}$ and 3F6-hIgG1$_{CHO}$ diluted in mouse plasma at a range of 1 to 500 ng/mL. Half-lives were calculated using $N_t = N_0\ (1/2)^{t/t1/2}$, where N_0 is the highest concentration of 3F6 antibodies, N(t) is the nondecayed concentration at time t, and t1/2 is the half-life of the decaying concentration.

Ethics Statement. Experiments with blood from human volunteers were performed with a protocol that was reviewed, approved, and supervised by the University of Chicago's Institutional Review Board (IRB). All mouse experiments were performed in accordance with the institutional guidelines following experimental protocol review and approval by the Institutional Biosafety Committee (IBC) and the Institutional Animal Care and Use Committee (IACUC) at the University of Chicago.

Data Availability. All data generated as part of this study are included in the article and *SI Appendix*.

ACKNOWLEDGMENTS. We thank Tatyana Golovkina, Vilasack Thammavongsa, and members of our laboratory for discussion. This project has been supported by funds from the National Institute of Allergy and Infectious Diseases, National Institutes of Health, Department of Health and Human Services, under Awards AI52474 and AI148543.

1. M. J. Kuehnert *et al*., Prevalence of *Staphylococcus aureus* nasal colonization in the United States, 2001-2002. *J. Infect. Dis.* **193**, 172–179 (2006).
2. A. van Belkum *et al*., Co-evolutionary aspects of human colonisation and infection by *Staphylococcus aureus*. *Infect. Genet. Evol.* **9**, 32–47 (2009).
3. C. von Eiff, K. Becker, K. Machka, H. Stammer, G. Peters, Nasal carriage as a source of Staphylococcus aureus bacteremia. Study Group. *N. Engl. J. Med.* **344**, 11–16 (2001).
4. R. S. Daum *et al*.; DMID 07-0051 Team, A placebo-controlled trial of antibiotics for smaller skin abscesses. *N. Engl. J. Med.* **376**, 2545–2555 (2017).
5. S. Y. Tong, J. S. Davis, E. Eichenberger, T. L. Holland, V. G. J. Fowler Jr., *Staphylococcus aureus* infections: Epidemiology, pathophysiology, clinical manifestations, and management. *Clin. Microbiol. Rev.* **28**, 603–661 (2015).
6. F. C. Lessa *et al*.; Active Bacterial Core surveillance (ABCs); MRSA Investigators of the Emerging Infections Program, Impact of USA300 methicillin-resistant *Staphylococcus aureus* on clinical outcomes of patients with pneumonia or central line-associated bloodstream infections. *Clin. Infect. Dis.* **55**, 232–241 (2012).
7. D. Missiakas, O. Schneewind, *Staphylococcus aureus* vaccines: Deviating from the carol. *J. Exp. Med.* **213**, 1645–1653 (2016).
8. F. Falugi, H. K. Kim, D. M. Missiakas, O. Schneewind, Role of protein A in the evasion of host adaptive immune responses by Staphylococcus aureus. *mBio* **4**, e00575-13 (2013).
9. E. Van Loghem, B. Frangione, B. Recht, E. C. Franklin, Staphylococcal protein A and human IgG subclasses and allotypes. *Scand. J. Immunol.* **15**, 275–278 (1982).
10. L. Zhang, K. Jacobsson, K. Ström, M. Lindberg, L. Frykberg, *Staphylococcus aureus* expresses a cell surface protein that binds both IgG and beta2-glycoprotein I. *Microbiology* **145**, 177–183 (1999).
11. H. K. Kim *et al*., Protein A-specific monoclonal antibodies and prevention of Staphylococcus aureus disease in mice. *Infect. Immun.* **80**, 3460–3470 (2012).
12. H. K. Kim, A. G. Cheng, H.-Y. Kim, D. M. Missiakas, O. Schneewind, Nontoxigenic protein A vaccine for methicillin-resistant Staphylococcus aureus infections in mice. *J. Exp. Med.* **207**, 1863–1870 (2010).
13. A. Forsgren, K. Nordström, Protein A from Staphylococcus aureus: The biological significance of its reaction with IgG. *Ann. N. Y. Acad. Sci.* **236**, 252–266 (1974).
14. A. Forsgren, A. Svedjelund, H. Wigzell, Lymphocyte stimulation by protein A of *Staphylococcus aureus*. *Eur. J. Immunol.* **6**, 207–213 (1976).
15. H. K. Kim, F. Falugi, D. M. Missiakas, O. Schneewind, Peptidoglycan-linked protein A promotes T cell-dependent antibody expansion during *Staphylococcus aureus* infection. *Proc. Natl. Acad. Sci. U.S.A.* **113**, 5718–5723 (2016).
16. N. T. Pauli *et al*., Staphylococcus aureus infection induces protein A-mediated immune evasion in humans. *J. Exp. Med.* **211**, 2331–2339 (2014).
17. H. K. Kim, F. Falugi, L. Thomer, D. M. Missiakas, O. Schneewind, Protein A suppresses immune responses during Staphylococcus aureus bloodstream infection in Guinea pigs. *mBio* **6**, e02369-14 (2015).
18. X. Chen, Y. Sun, D. Missiakas, O. Schneewind, Staphylococcus aureus decolonization of mice with monoclonal antibody neutralizing protein A. *J. Infect. Dis.* **219**, 884–888 (2019).
19. V. Thammavongsa, S. Rauch, H. K. Kim, D. M. Missiakas, O. Schneewind, Protein A-neutralizing monoclonal antibody protects neonatal mice against Staphylococcus aureus. *Vaccine* **33**, 523–526 (2015).
20. R. Jefferis, Glycosylation as a strategy to improve antibody-based therapeutics. *Nat. Rev. Drug Discov.* **8**, 226–234 (2009).
21. L. X. Wang, J. V. Lomino, Emerging technologies for making glycan-defined glycoproteins. *ACS Chem. Biol.* **7**, 110–122 (2012).
22. L. X. Wang, M. N. Amin, Chemical and chemoenzymatic synthesis of glycoproteins for deciphering functions. *Chem. Biol.* **21**, 51–66 (2014).
23. W. Huang, J. Giddens, S. Q. Fan, C. Toonstra, L. X. Wang, Chemoenzymatic glycoengineering of intact IgG antibodies for gain of functions. *J. Am. Chem. Soc.* **134**, 12308–12318 (2012).
24. T. Li, X. Tong, Q. Yang, J. P. Giddens, L. X. Wang, Glycosynthase mutants of endoglycosidase S2 show potent transglycosylation activity and remarkably relaxed substrate specificity for antibody glycosylation remodeling. *J. Biol. Chem.* **291**, 16508–16518 (2016).
25. I. Quast *et al*., Sialylation of IgG Fc domain impairs complement-dependent cytotoxicity. *J. Clin. Invest.* **125**, 4160–4170 (2015).
26. G. P. Subedi, A. W. Barb, The immunoglobulin G1 N-glycan composition affects binding to each low affinity Fc γ receptor. *MAbs* **8**, 1512–1524 (2016).
27. C. A. Diebolder *et al*., Complement is activated by IgG hexamers assembled at the cell surface. *Science* **343**, 1260–1263 (2014).
28. M. Hezareh, A. J. Hessell, R. C. Jensen, J. G. van de Winkel, P. W. Parren, Effector function activities of a panel of mutants of a broadly neutralizing antibody against human immunodeficiency virus type 1. *J. Virol.* **75**, 12161–12168 (2001).
29. A. J. Hessell *et al*., Fc receptor but not complement binding is important in antibody protection against HIV. *Nature* **449**, 101–104 (2007).
30. J. R. Gasdaska, S. Sherwood, J. T. Regan, L. F. Dickey, An afucosylated anti-CD20 monoclonal antibody with greater antibody-dependent cellular cytotoxicity and B-cell depletion and lower complement-dependent cytotoxicity than rituximab. *Mol. Immunol.* **50**, 134–141 (2012).
31. F. Nimmerjahn, P. Bruhns, K. Horiuchi, J. V. Ravetch, FcgammaRIV: A novel FcR with distinct IgG subclass specificity. *Immunity* **23**, 41–51 (2005).
32. L. Thomer, O. Schneewind, D. Missiakas, Pathogenesis of *Staphylococcus aureus* bloodstream infections. *Annu. Rev. Pathol.* **11**, 343–364 (2016).
33. S. A. Plotkin, Vaccines: Correlates of vaccine-induced immunity. *Clin. Infect. Dis.* **47**, 401–409 (2008).
34. H. Rus, C. Cudrici, F. Niculescu, The role of the complement system in innate immunity. *Immunol. Res.* **33**, 103–112 (2005).
35. S. H. E. Kaufmann, Immunology's coming of age. *Front. Immunol.* **10**, 684 (2019).
36. L. L. Lu, T. J. Suscovich, S. M. Fortune, G. Alter, Beyond binding: Antibody effector functions in infectious diseases. *Nat. Rev. Immunol.* **18**, 46–61 (2018).
37. H. Kaplon, J. M. Reichert, Antibodies to watch in 2019. *MAbs* **11**, 219–238 (2019).
38. N. W. van de Donk *et al*., Monoclonal antibodies targeting CD38 in hematological malignancies and beyond. *Immunol. Rev.* **270**, 95–112 (2016).
39. G. J. Weiner, Building better monoclonal antibody-based therapeutics. *Nat. Rev. Cancer* **15**, 361–370 (2015).
40. D. Ricklin, G. Hajishengallis, K. Yang, J. D. Lambris, Complement: A key system for immune surveillance and homeostasis. *Nat. Immunol.* **11**, 785–797 (2010).
41. J. R. Dunkelberger, W. C. Song, Complement and its role in innate and adaptive immune responses. *Cell Res.* **20**, 34–50 (2010).
42. M. Butler, M. Spearman, The choice of mammalian cell host and possibilities for glycosylation engineering. *Curr. Opin. Biotechnol.* **30**, 107–112 (2014).
43. C. Ferrara *et al*., Unique carbohydrate-carbohydrate interactions are required for high affinity binding between FcgammaRIII and antibodies lacking core fucose. *Proc. Natl. Acad. Sci. U.S.A.* **108**, 12669–12674 (2011).

Downloaded at Palestinian Territory, occupied on December 30, 2021

www.manaraa.com

44. L. Malphettes *et al*., Highly efficient deletion of FUT8 in CHO cell lines using zinc-finger nucleases yields cells that produce completely nonfucosylated antibodies. *Biotechnol. Bioeng.* **106**, 774–783 (2010).
45. G. Dekkers *et al*., Decoding the human immunoglobulin G-glycan repertoire reveals a spectrum of Fc-receptor-and complement-mediated-effector activities. *Front. Immunol.* **8**, 877 (2017).
46. Y. Kaneko, F. Nimmerjahn, J. V. Ravetch, Anti-inflammatory activity of immunoglobulin G resulting from Fc sialylation. *Science* **313**, 670–673 (2006).
47. D. A. C. Heesterbeek, M. L. Angelier, R. A. Harrison, S. H. M. Rooijakkers, Complement and bacterial infections: From molecular mechanisms to therapeutic applications. *J. Innate Immun.* **10**, 455–464 (2018).
48. V. Thammavongsa, H. K. Kim, D. Missiakas, O. Schneewind, Staphylococcal manipulation of host immune responses. *Nat. Rev. Microbiol.* **13**, 529–543 (2015).
49. N. Shushakova *et al*., C5a anaphylatoxin is a major regulator of activating versus inhibitory FcgammaRs in immune complex-induced lung disease. *J. Clin. Invest.* **110**, 1823–1830 (2002).
50. S. N. Syed *et al*., Both FcgammaRIV and FcgammaRIII are essential receptors mediating type II and type III autoimmune responses via FcRgamma-LAT-dependent generation of C5a. *Eur. J. Immunol.* **39**, 3343–3356 (2009).
51. Q. Zhou *et al*., Development of a simple and rapid method for producing non-fucosylated oligomannose containing antibodies with increased effector function. *Biotechnol. Bioeng.* **99**, 652–665 (2008).
52. M. Yu *et al*., Production, characterization and pharmacokinetic properties of antibodies with N-linked Mannose-5 glycans. *MAbs* **4**, 475–487 (2012).
53. R. Wada, M. Matsui, N. Kawasaki, Influence of N-glycosylation on effector functions and thermal stability of glycoengineered IgG1 monoclonal antibody with homogeneous glycoforms. *MAbs* **11**, 350–372 (2019).
54. H. K. Kim, V. Thammavongsa, O. Schneewind, D. Missiakas, Recurrent infections and immune evasion strategies of *Staphylococcus aureus*. *Curr. Opin. Microbiol.* **15**, 92–99 (2012).
55. P. A. Longo, J. M. Kavran, M.-S. Kim, D. J. Leahy, Transient mammalian cell transfection with polyethylenimine (PEI). *Methods Enzymol.* **529**, 227–240 (2013).

Downloaded at Palestinian Territory, occupied on December 30, 2021

www.manaraa.com